Demographically Stuck by Climate Change: Sea-Level Rise Migration in the United States.

Mathew E. Hauer[a,1,2], **Sunshine Jacobs**[a,b], **and Scott A. Kulp**[c]

[a]Department of Sociology, Florida State University; [b]Center for Demography and Population Health, Florida State University; [c]Climate Central

This manuscript was compiled on October 18, 2021

The warnings of sea-level rise (SLR) driven migration first appeared in the scientific literature in the late 1970s when increased recognition that disintegrating ice sheets could drive people to migrate from coastal cities. Since that time, scientists have modelled potential SLR driven migration without integrating other population processes, potentially obscuring the total demographic impact of SLR migration. If sea-level rise forces millions of people further inland, a potential domino effect could result, further enhancing migration to more distant locations and further suppressing migration to coastal areas. Older populations are also the least likely to migrate and SLR migration could accelerate population aging in coastal areas. Here, we investigate both the potential domino effect of SLR migration and the potential emergence of "demographically stuck" populations by combining matrix population models, flood hazard models, and a machine learning model built on 40 years of environmental migration in the US to project the US population distribution of US counties, accounting for anticipated demographic change, migration probabilities, and sea-level rise. We find that the total demographic impact of 0.9m of SLR in 2100 is nearly 13 million people – four times the number of migrants – under SSP2 and the 95h percentile of RCP4.5. We project a significant "hollowing" of coastal age structures as youthful populations migrate but older populations remain. The potential for "demographically stuck" populations has received scant attention but could occur in heavily impacted areas. Furthermore, our population projection approach can be easily adapted to investigate additional or multiple climate hazards.

Climate Migration | Sea-level Rise | Demography | Multiregional Population Projections

Scientists first sounded the alarm of potential "major dislocations in coastal cities" (1) due to a disintegrating West Antarctic Ice Sheet and sea-level rise more than forty years ago. Since those early warnings, experts continue to regard sea-level rise as one of the most costly and visible future impacts of global climate (2–4). With the global coastal population projected to eclipse one billion people this century (5), sea-level rise is expected to affect and, in many cases, displace hundreds of millions of people (3, 6).

While the scientific community understands that climate change and sea-level rise will affect millions of people in the United States and across the world, we face a critical knowledge gap about the impacts of rising sea levels on human migration. Previous attempts to model sea-level rise and migration eschew two key considerations.

First, scientists have chosen to model migrants as age-less and sex-less individuals (6–9), ignoring the well-established relationship between migration propensity and demographic characteristics (10–12). In particular, the near universal age schedule of migration, with older populations the least likely age groups to migrate and young adults the most (**Figure 1**), suggests SLR migration is most likely to occur among working-age adults. The age schedule of migration in conjunction with the anticipated global, demographic shift toward a considerably older population at the end of the century (13), suggests the potential emergence of "demographically stuck" people. By ignoring these well-established demographic relationships, the extent to which highly vulnerable coastal communities could experience accelerated population aging as more youthful populations migrate away remains unknown.

Second, sea-level rise migration models lack the crucial feedback loop whereby sea-level rise migrants alter the demographic trajectory in both their origin and destination. If sea-level rise forces millions of people further inland, a potential domino effect could result, further enhancing population growth in more distant locations and further suppressing population growth to coastal areas (14–16). [WHAT DOES THIS CAUSE US TO MISS?]

In this paper, we combine matrix population models, flood hazard models, and a migration model built on 40 years of environmental migration to project the United States' population distribution, accounting for anticipated demographic change, migration probabilities, and sea-level rise. This approach allows us to investigate the potential for accelerated aging in coastal communities and the potential for "demographically trapped" peoples and the temporal and demographic dimensions of anticipated sea-level rise migration.

To investigate SLR migration, we produce three separate population populations using a multi-regional Leslie matrix that takes the following general form

$$\mathbf{P_{t+1}} = \underbrace{\underbrace{\mathbf{M_t}(\hat{\mathbf{S}}_\mathbf{t}\mathbf{P_t} - \overbrace{\mathbf{S_tP_t}}^{Base})}_{Inundation} + \hat{\mathbf{S}}_\mathbf{t}\mathbf{P_t}}_{Migration} \quad [1]$$

Where $\mathbf{P_{t+1}}$ is the population at time $t+1$, $\mathbf{S_t}$ is a Leslie matrix containing the age-sex specific probabilities of fertility

Significance Statement

Authors must submit a 120-word maximum statement about the significance of their research paper written at a level understandable to an undergraduate educated scientist outside their field of speciality. The primary goal of the Significance Statement is to explain the relevance of the work in broad context to a broad readership. The Significance Statement appears in the paper itself and is required for all research papers.

Please provide details of author contributions here.

The authors declare no conflict of interest.

[1] A.O.(Author One) and A.T. (Author Two) contributed equally to this work (remove if not applicable).

[2] To whom correspondence should be addressed. E-mail: mehauer@fsu.edu

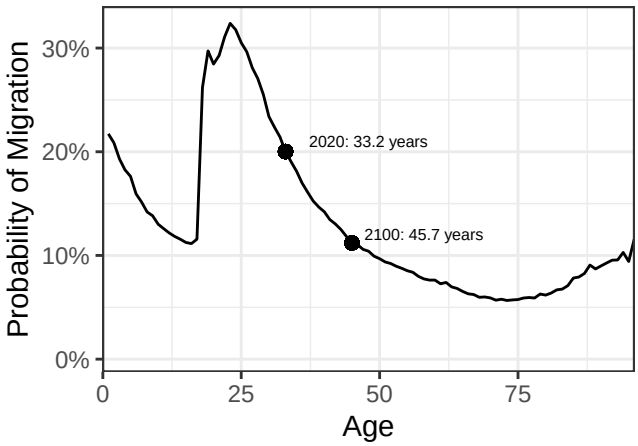

Fig. 1. Probability of Migrating by Age and Median Age in 2020 and 2100 in the United States. Figure generated using IPUMS-USA data (17). Median age is calculated based on Shared Socioeconomic Pathway 2 (18). Barring any additional information, this curve suggests that migration will lessen as the US population ages this century.

and survival, $\hat{\mathbf{S}}_t$ is a Leslie matrix populated with the results of a displacement model, and $\mathbf{M}_t$ is a matrix containing the probability of migrating from county i to county j.

We derive three population projections. $\mathbf{S_tP_t}$ is our `Base` population projection and represents a projection agnostic to climate change. $\hat{\mathbf{S_t}}\mathbf{P_t} - \mathbf{S_tP_t}$ is our `Inundation` projection, representing a similar projection to those undertaken in the broader literature (e.g. (7, 9, 19). Our full model, which we refer to as `Migration`, accounts for population dynamics in origins and destinations.

We populate our matrices from multiple data sources. $\mathbf{P_t}$ come from the National Vital Statistics System (NVSS) U.S. Census Populations with Bridged Race Categories Dataset. $\mathbf{M_t}$ contains the probability of migrating from each county to each county based on the IRS county-to-county migration data. The annual series of county-to-county migration data cover 95 to 98 percent of the tax-filing universe (or approximately 87% of US households (20)) and their dependents making these data the largest migration data source for count flows between counties in the United States. Finally, $\mathbf{S_t}$ and $\hat{\mathbf{S}}\mathbf{t}$ are populated with cohort-change ratios (CCRs) from the NVSS population data.

$\hat{\mathbf{S}}_\mathbf{t}$ contains the same information as $\mathbf{S_t}$ but reduced based on the percentage of population we anticipate will be displaced by SLR. We arrive at this reduction with a simple, parsimonious model fit with US counties between 1980 and 2018 with SHELDUS verified large ($>4\sigma$) population declines (n=48 such county-years). We estimate exposure to SLR as a percentage of the population in each county using a bathtub model of inundation based on the population-weighted area under the 95th percentile of RCP4.5 (for a 2100 SLR amount of ~0.9M). All population results are reported based on SSP2.

Finally, $\mathbf{M_t}$, $\mathbf{S_t}$, and $\hat{\mathbf{S}}_\mathbf{t}$ are projected forward using ARIMA(0,1,1) ($\mathbf{S_t}$ and $\hat{\mathbf{S}}_\mathbf{t}$) and ETS models ($\mathbf{M_t}$) to capture potential changes in demographic rates.

Results

We find that 0.9m of SLR compromises the land area home to 3.4 million people between 2020 and 2100. In this simple model, the demographic impact of SLR is 3.4 million people migrating to other places for a net demographic change of just 3.4 million people. However, when one accounts for population dynamics, the actual *demographic* impact of 3.4 million migrants is 12.96 million people. This is due to the population momentum we expect to occur due to the interacting effects of basic demographic component processes of migration, fertility, and mortality. Most surprising is that this demographic effect is considerably more pronounced than the simple displacement effect – in fact, it is nearly four times larger!

Furthermore, **Figure 2** shows this population momentum effect for example nine counties following the general typology of climate migration put forth by (16). Here, the three counties in the 'Vulnerable Counties' (those most exposed to a climate hazard) all experience considerably pronounced demographic declines, even with rather marginal displacements. In the case of Miami-Dade, 0.9m of SLR suggests 251K migrants by 2100 but a total demographic impact of 1.4M people. The same larger total demographic impact compared to simple displacement is also present in Beaufort () and Poquoson ().

In the 'Climate Destinations' (counties considered 'climate havens'), we see a similar, though reversed, pattern of population trajectories to 'Vulnerable Counties.' Here, Place CA (home to Lake Tahoe), Buncombe NC (home to Asheville), and Erie NY (home to Buffalo), all exhibit considerably larger demographic impacts when accounting for population dynamics compared to just a simple displacement model. In the case of Erie NY, this finding echoes many suggestions that Buffalo might become a climate haven this century [CITES].

In the 'Recipient Counties' (counties closest to heavily threatened counties), we see three separate population trajectories and demonstrates the non-linearity in population change. West Baton Rouge, threatened by SLR early this century, appears to be a Vulnerable County until the middle of the century, where population momentum carries it below an anticipated projection without SLR. Yet by the tail end of the century, West Baton Rouge's population momentum carries it above even a climate agnostic projection, suggesting it transitions into a Climate Destination. Given the extreme precarity of coastal Louisiana, West Baton Rouge and similar nearby Louisiana Parishes could transition from Vulnerable to Climate Destination.

This is in stark contrast to Broward FL, immediately north of Miami-Dade, and Queens NY. Here, both counties appear as climate destinations in the early part of the century. But SLR also threatens Broward and Queens and demographic change turns sharply negative in the latter part of this century. Unlike West Baton Rouge, these counties could initially be a Climate Destination only to turn into a Vulnerable County as the century progresses. These results suggest that many people and their descendants could find themselves exposed and displaced by SLR as presently safe areas become increasingly vulnerable over time.

Figure 3 shows the impact of population processes on aging related to climate migration. We find that as the percentage of the population lost due to climate migration-related population processes increases, the median age in the population also increases (**Figure 3a**). Conversely, counties receiving the greatest increase actually exhibit more *youthful* populations. This effect is particularly pronounced in some counties where the increase in median age can approach +12 years in some

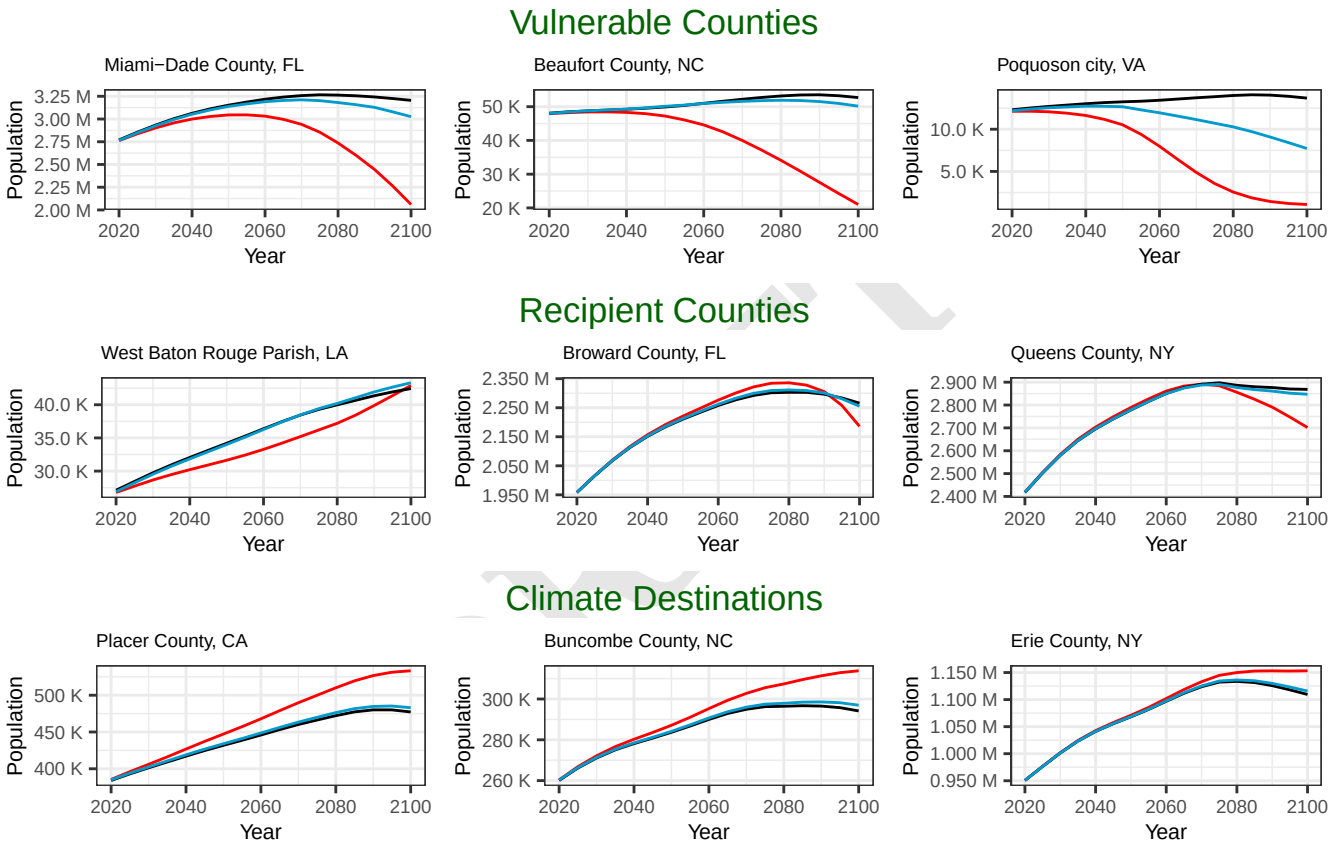

Fig. 2. A comparison of base, inundation, and migration projections for four sample counties over the next century with 3ft of SLR. We adopt the general climate migration typology as proposed by (**?**). The inundation model projection refines the previous base model as it accounts for sea-level rise displacement. Including demographic processes further sophisticates the migration projection. In the case of these example counties, the migration model reflects both those who emigrated and their lost progeny, indicating a substantial decline in the projected population for 2100 as compared to the base model population.

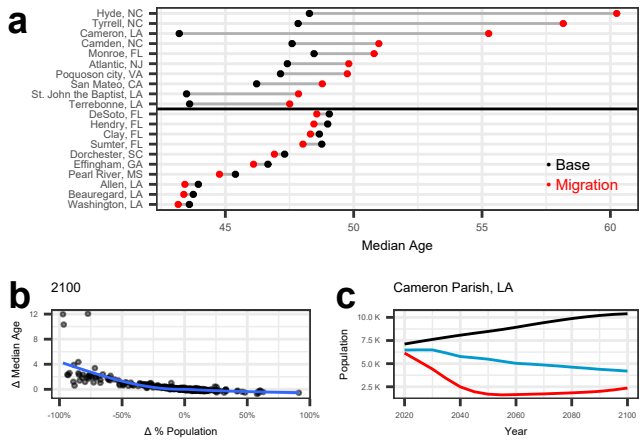

Fig. 3. Population Aging and 'Demographically Stuck' populations. (a) shows the ten counties with the most and least aging due to SLR migration. (b) shows the relationship between population decline due to SLR and aging by 2100. (c) shows an example of a county with demographically stuck people.

highly impacted coastal counties due to SLR migration.

We also find an example of how these three processes – population aging, reduced propensity to migrate among older populations, and SLR migration – combine to potentially create 'demographically stuck' populations. **Figure 3b** shows one such county, Cameron Parish LA. Here, a climate agnostic population projection shows the county slowly gaining population this century and a simple inundation model shows the county steadily losing population. However, the fully integrated population model suggests a striking, non-linear potential population pathway. The parish rapidly loses population until the middle of the century, before slowly increasing in population, eventually yielding a larger population in 2100 compared to the simple inundation model. We believe this is emblematic of the potential for emerging, 'demographically stuck' populations that more simplistic displacement models will miss.

Figure 4 shows this increased aging across space and reveals several important patterns. First, most coastal counties see increased population aging by 2100 and most coastal-adjacent counties will experience a more youthful population compared to a demographically agnostic projection. Most migration operates within kin and social networks within relatively short-distances and across pre-existing migration pathways (21). Second, SLR impacts are hyperlocalized with the majority of heavy population aging limited to select areas in Louisiana, the Outer Banks of North Carolina, and the San Francisco Bay Area. And Third, additional non-linearity emerges as some coastal counties can experience reverse aging and some inland counties can experience aging due to climate migration.

Discussion

We Discuss that

Conclusion

We Discuss that

Materials and Methods. To answer our research questions, we employ three main modules. The first is the development of a parsimonious, one-dimensional, age-specific displacement model. The second is a multiregional Leslie matrix specification. The third is a sea-level rise exposure model.

Parimonious, one-dimensional, age-specific displacement model. Our displacement model makes use of a statistical time series outlier detection technique to first identify anomalous demographic behavior in a time series and then verify that this anomalous behavior is associated with an environmental event.

We use a statistical time series outlier detection algorithm (22), implemented in the R programming language (23) via the tsoutliers package (24).

This algorithm iteratively uses ARIMA models to 1) identify potential outliers and 2) refit the ARIMA with the outliers removed to produce a counter-factual time series. First, an ARIMA model is fit to the time series using the `forecast` package in R (25, 26) where the best performing ARIMA model is selected based on the Bayesian information criterion (BIC). Finally, the residuals from the forecast are checked for their significance where only outliers above a critical t-static are considered "true" outliers ($|\tau| \geq 4$; p-value < 0.000063). We chose this threshold to minimize the probability of committing a Type I error (or claiming an outlier is true when it is, in fact, not).

We use this outlier detection algorithm to search over county population totals for the time period 1980-2018. We use the National Vital Statistics System (NVSS) U.S. Census Populations with Bridged Race Categories data set. The NVSS Bridged Race Categories data set harmonizes racial classifications across disparate time periods to allow population estimates to be sufficiently comparable across space and time. Importantly, all county boundaries are rectified to be geographically consistent across all time periods. We use the the 1969-2018 dataset, but the historical population estimates prior to 1980 display unusual volatility, so we consider only the time periods 1980-2018. We also only consider counties created prior to year 2000 and contained in the NVSS data.

We search all US counties for negative statistical outliers (indicating population losses) between 1980 and 2018. We detect 52 county-years with population losses of magnitude 4σ or greater (see **Supplementary Table X** for the details of these county-years). We then use the Spatial Hazard Events and Losses Database for the United States (SHELDUS) (27), a county-level hazard data set for the US which contains information about the direct losses (property and crop losses, injuries, and fatalities) caused by a hazard event (thuderstorms, hurricanes, floods, wildfires, tornados, flash floods, earthquakes, etc.) for the period 1960 to the present. We use SHELDUS to ensure the county time periods we identify as statistical outliers with population losses experienced an environmental hazard in that county-year with per capita hazardous losses in excess of the 50th percentile. This is to ensure the outlier population losses that we detect are associated with a hazard rather than other forces, such as economic forces.

Four county-periods either were not in the SHELDUS database or experienced per capita hazard losses below the 50th percentile. Additionally, one county-period contained age-sex groups with 0 people, necessitating exclusion. The remaining 48 environmental events include tornados, wind

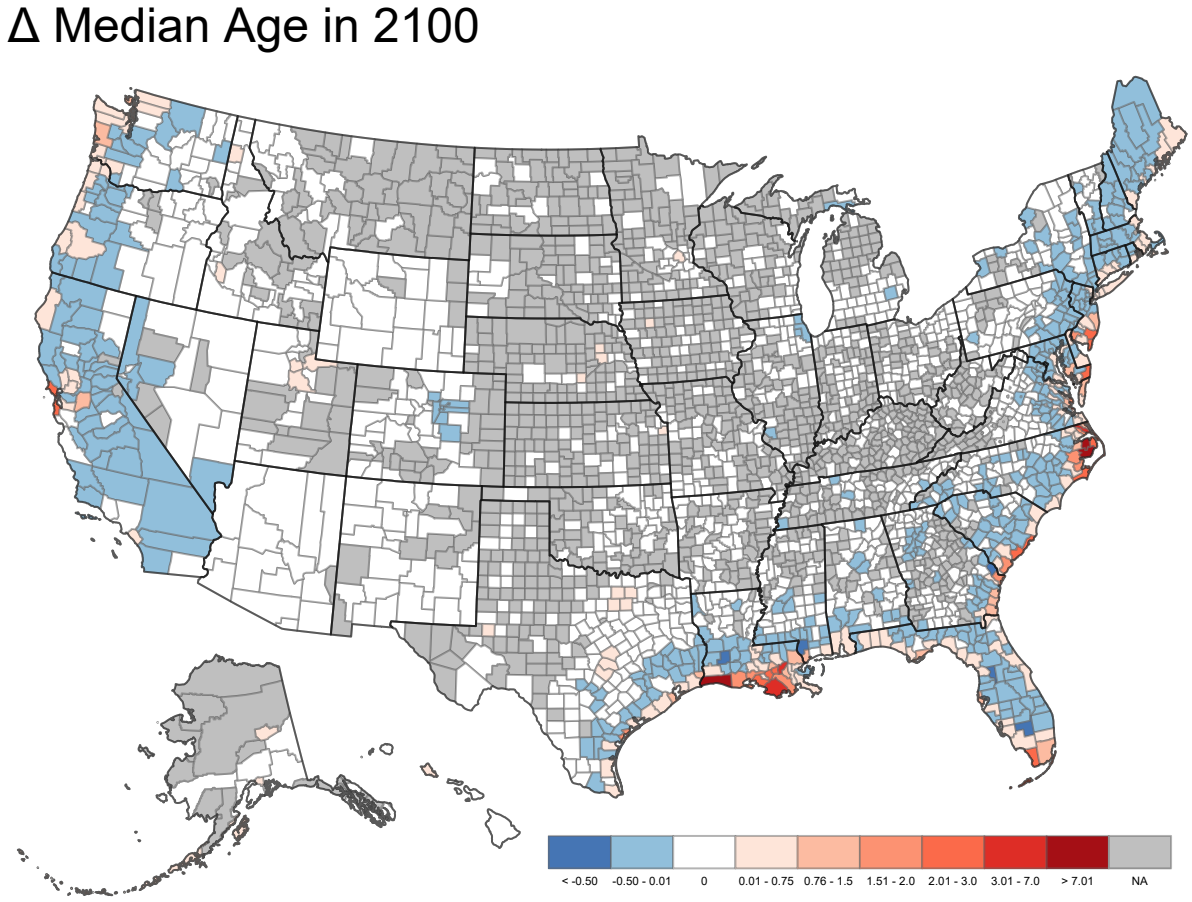

Fig. 4. A comparison of base, inundation, and migration projections for four sample counties over the next century with 3ft of SLR. Additional caption.

damage, winter weather, earthquakes, flooding, tropical cyclones, hail, and other environmental hazards. Using this universe of 48 county-periods exhibiting large population declines after verified hazard losses, across over 40 years and across a wide variety of environmental hazards, we then build a flexible, one-dimensional, age-specific displacement model.

To link population displacement with age-specific population changes, we calculate cohort-change ratios (CCRs) in each county using the NVSS population data for the period 1969-2018. Cohort-change ratios take the following general form (see (28, 29) for a more detailed description):

$$CCR_{x,t} = \frac{{}_nP_{x,t}}{{}_nP_{x-y,t-y}} \quad [2]$$

Where ${}_nP_{x,t}$ is the population aged x to $x+n$ in time t and ${}_nP_{x-y,t}$ is the population aged $x-y$ to $x+n-y$ in time t where y refers to the time difference between time periods. Since mortality must decrement a population, any CCR above 1.0 implies a net-migration rate in excess of the mortality rate, and a growing population.

We build the following model based on the relationship between the change in CCRs at age x, $\Delta CCR_x = CCR_{x,t}/CCR_{x,t-1}$, and the percentage decline in the total population compared to the counter-factual in the outlier detection method, $\Delta P_t = \hat{P}_t/P_t$:

$$log(\Delta CCR_x) = a_x + b_x h \quad [3]$$

Here, h is the $\log(\Delta P_t)$ and shows a linear relationship with the logarithm of the change in CCRs by age. x refers to five-year age groups: 0-4, 5-9,..., 85+. This is a similar model and approach to Wilmoth et al.'s (30) flexible, one-dimensional mortality model based on the linearity between age-specific mortality rates and infant mortality. **Supplementary Table 1** depicts the correlation coefficients between $\log(\Delta CCR_x)$ and $\log(\Delta P_t)$. The age groups with the lowest correlation coefficients are young adult males aged 20-39 and those in the open-ended age interval (80+), suggesting these age/sex groups react to environmental signals the least predictably.

Using $h = log(\Delta P_t)$, we can estimate age-specific changes in CCRs after an environmental event by simply applying the following formula:

$$\hat{CCR}_{x,t} = CCR_{x,t-1} \cdot e^{\hat{\beta}_x h} \quad [4]$$

Where $e^{\hat{\beta}_x h}$ provides the percentage change in CCR_x based on the $\log(\Delta P_t)$.In this case, we drop the intercept (a) from the estimation procedure to ensure a 0% decline in population yields a corresponding 0% change in the CCR. Multiplying the result from the model with the CCR in the year prior yields the anticipated change in the CCR. These changes in CCRs can then be applied to any time series of population values to generate an anticipated population.

We estimate the predicted population using the equation outlined above and then compare it against the observed population. **Supplementary Figure 1** shows the accuracy of our fitted, one-dimensional model. Regarding the total population in our 48 counties, our model performs well with an r^2 value of 0.994 and performs well regardless of population size. Regarding each individual P_x group, our model still performs quite well with an r^2 of 0.976. Just like with the total population, the accuracy of our model does not depend on population size.

Sea-level Rise Exposure. To estimate the populations at-risk to SLR and thus the value h in *Equation 4*, we employ inundation modeling (15) which assumes that people who are underwater 100% of the time must migrate. We estimate these populations using airborne lidar-derived digital elevation models (DEMs) produced by NOAA and supplemented with both the USGS Northern Gulf of Mexico Topobathymetric DEM in Louisiana and the USGS National Elevation Dataset in the fraction of land not covered by other sources (see (31) for details on the construction of the DEMs).

Using a bathtub model of inundation, we calculate the land area under a given water height to generate binary inundation surfaces. SLR exposure is hyperlocalized, and we generate this inundation area in the Census Block Groups (CBG; n=81,815) located in coastal counties (n=406) expected to experience any probability of flooding. We use probabilistic SLR projections (32, 33) that are closely aligned with the IPCC for our water heights. To calculate the land area under a given water height, we simply threshold the DEM to find pixels below SLR_{yt} where y is the projected height of SLR in a given year t. For each CBG, we simply calculate the percentage of its pixels on dry land (defined in the National Wetland Inventory (34)) covered by the inundation surface and multiply this percentage by the total population in the CBG in year t to produce the total number of people at-risk to a given amount of SLR in a given year. We then aggregate these CBGs to the county-level to calculate the percentage of people in a given county at-risk of inundation.

To account for potential sub-county shifts in population, we use a sub-county demographic projection to produce spatiotemporally consistent CBG boundaries for the period 1940-2010 and project these populations forward using a mixed, linear/exponential projection for the period 2010-2100. We use the 'Year Structure Built' question from the 2013-2018 US Census Bureau's ACS to calculate the number of housing units H in each CBG. We calculate H in th eperiod 1940-2010 using $\hat{H}^v_{ij} = \left(\frac{C^v_j}{\sum_{i=1}^{n}\sum_{t=1939}^{v-1} H^v_{ijt}}\right) \cdot \sum_{t=1939}^{v-1} H^v_{ijt}$, where C^v_j is the number of HUs in county j counted in census taken in time v, H^v_{ij} is the number of HUs in block group i in county j based on the "year structure built" question in the ACS, and v is the set of time periods $v \in \{1940, 1950, 1960, 1970, 1980, 1990, 2000, 2010\}$. We then project these housing unit values using a linear projection for any CBG experiencing population growth and an exponential projection for any CBG experiencing population decline. See (35, 36) for more details.

We convert H to population P via the Housing Unit Method of population estimation ($P_t = H \cdot PPHU$) where the population is given as the number of people per housing unit ($PPHU$) multiplied by the number of housing units (H). Using a similar approach as estimating H, we estimate the population in each time period with $P'^v_{ij} = \frac{P^v_j}{\sum\left[\left(\frac{PPHU^{2018}_{ij}}{PPHU^{2018}_{j}} \cdot PPHU^v_j\right) \cdot \hat{H}^v_{ij}\right]} \cdot \hat{P}^v_{ij}$ where the $PPHU$ in 2018 from the ACS is denoted as $PPHU^{2018}_{ij}$ while the $PPHU$ observed in in historical time v from historical census data is denoted as $PPHU^v_j$.

To calculate the percentage of the population at-risk in each county, we multiply the percentage of each CBG inundated under a given water height y in time period t by P'^t_{ij} to produce

P_{ij}^{risk}. The ratio of the total population ($\sum P_{ij}^{risk}/P_j^{'t}$) in each county in year t is thus the percentage of the population in a given county at-risk of inundation.

The percentage of the population at-risk to SLR in each county, in essence, represents the ΔP_t from our equations above where $\Delta P_t = \hat{P}_t/P_t$. In this case, $\hat{P}_t/P_t$ is the percentage of the population in any county at-risk of inundation. Such a calculation allows us to seamlessly combine our parsimonious displacement model with our matrix population model.

Matrix Population Models We employ the use of multiregional leslie matrices in our population projections (37).

In a typical Leslie matrix,

$$\mathbf{P_{t+1}} = \mathbf{S_t} \cdot \mathbf{P_t} \quad [5]$$

Where $\mathbf{P_t}$ refers to the population matrix containing k age groups and $\mathbf{S_t}$ contains the age-specific fertility and mortality rates.

Thus, to produce a population projection, the operation looks akin to

$$\begin{bmatrix} 0 & F_2 & F_3 \\ S_1 & 0 & 0 \\ 0 & S_2 & S_3 \end{bmatrix} \cdot \begin{bmatrix} P_1 \\ P_2 \\ P_3 \end{bmatrix} = \begin{bmatrix} 0 & 0.2 & 0.2 \\ 0.62 & 0 & 0 \\ 0 & 0.35 & 0.35 \end{bmatrix} \cdot \begin{bmatrix} 100 \\ 100 \\ 100 \end{bmatrix} = \begin{bmatrix} 40 \\ 68 \\ 71 \end{bmatrix}$$

In a multi-regional projection model, we can use a "supermatrix."

A 2-region model would take the following general form for the $\mathbf{S_t}$ matrix,

$$\mathbf{MS_{t+1}} = \left[\begin{array}{c|c} \mathbf{S_i} & \mathbf{M_{j\to i}} \\ \hline \mathbf{M_{i\to j}} & \mathbf{S_j} \end{array}\right]$$

Such that the diagonal $\mathbf{S}$ matrices contain combined survival, fertility, and migration probabilities while the off-diagonal $\mathbf{M}$ matrices contain the probabilities of each age-group moving from one region to the other.

We populate our Leslie matrices with the 3,143 US counties, 18 five-year age groups, and two sex groups. We use CCRs to populate our S values in each matrix and child-woman ratios to populate our F values. The values come from the NVSS Bridged Race Categories. To project the CCRs, We employ an autoregressive integrated moving average (ARIMA) model for forecasting equally spaced univariate time series data. We use an `ARIMA(0,1,1)` model, which produces forecasts equivalent to simple exponential smoothing. All projections were undertaken in **R** (23) using the `forecast` package (25).

We use the NVSS data for the period 1969-2018 for county c, age group x, sex s in an `ARIMA(0,1,1)` to create CCR_{cxst} for time periods $t+1$. The initial $\mathbf{P_1}$ and $\mathbf{S_t}$ matrices use the 2018 NVSS data. CCR_{cxst} is reduced using equation (4) where h is the percentage of the population at-risk to SLR in order to populate the $\hat{\mathbf{S}}_\mathbf{t}$ matrix.

We also calculate the probability of migrating from each county to each county and use this to populate the $\mathbf{M_t}$ matrix. These data come from the IRS county-to-county migration files from 1990-2018 (see (38) and (39) for descriptions of this data). The IRS began using tax data to estimate migration in the 1970s and 1980s (40, 41) and began releasing migration data in 1990. The IRS uses individual federal tax returns, matches these individual returns between two tax years (for instance, tax year 2000 and tax year 2001), and identifies both migrants and non-migrants. Beginning with the tax year 1991 (the migration year 1990), the IRS produces these data in conjunction with the US Census Bureau using the IRS Individual Master File, which contains every Form 1040, 1040A, and 1040EZ (42). We identify migration when a current years' tax form contains an address different from the preceding years' return. A non-migrant is identified when there is no change in address between two years. For the 2002 tax year, the IRS migration data contained approximately 130 million returns (42).

The annual series of county-to-county migration data cover 95 to 98 percent of the tax-filing universe (or approximately 87% of US households (20)) and their dependents making these data the largest migration data source for count flows between counties in the United States. The IRS derives migration information from tax-filings making those who do not file taxes most likely to be underrepresented in the migration data (42, 43), namely undocumented populations, the poor, the elderly, and college students (42). However, the overwhelming majority of householders file US tax returns in the United States (20).

To capture changes in the migration system, we employ an ETS model (Error, Trend, Seasonal), a univariate time series forecasting model (44). We use an ETS model for migration instead of an ARIMA(0,1,1) as we do for the CCRs because the CCRs are subject to multiplication during a drift, whereas the migration system is not. A CCR that drifts from 1.1 $\rightarrow$ 1.3 represents more than a 10-fold increase in a projected population over our time horizons (1.1^17 = 5x, 1.3^17 = 86x). Projecting the migration system itself is not subject to such exponential drift.

We fit individual ETS models for each county's numeric migrants between each origin-destination dyadic pair using the `forecast` package in R (25). This approach allows the underlying migration system to evolve and change over the projection horizon, allowing dyadic pairs to wax or wane.The model converts the numeric projections to fractions of the total projected migrants to populate the diagonal in the $\mathbf{M}$ matrix above where non-migrants (i.e. those migrating from $i \rightarrow i$) are included. The result is the fraction of individuals surviving from age group a who migrate from $i \rightarrow j$.

The $\mathbf{M_t}$ matrix takes the following general form

$$\mathbf{M_t} = \left[\begin{array}{ccc|ccc} 1 & 0 & 0 & 0 & 0 & 0 \\ 0 & 0.85 & 0 & 0 & 0 & 0 \\ 0 & 0 & 1 & 0 & 0 & 0 \\ \hline 0 & 0 & 0 & 1 & 0 & 0 \\ 0 & 0.15 & 0 & 0 & 1 & 0 \\ 0 & 0 & 0 & 0 & 0 & 1 \end{array}\right] \quad [1]$$

Where the migration rate from i to j in age group 2 is 0.15.

We control all population projections to the Shared Socioeconomic Pathway 2: Middle of the Road (18) and we use the 95th percentile of RCP4.5 for our inundation scenario (45). Full results for all plausible SSP/RCP combinations are available in the **Supplementary Material**.

Data Availability. The data resulting from this study are deposited at 10.5281/zenodo.5562904 [CITE]. The underlying data that support the findings of this study are available from Climate Central but restrictions apply to the availability of these data, which were used under license for the current study, and so are not publicly available. Data are however available from the authors upon reasonable request and with permission

of Climate Central.

Code Availability. Code to reproduce our analysis is available at 10.5281/zenodo.5562904 [CITE].

Acknowledgments. This work was supported by the State of Louisiana, the American Society of Adaptation Professionals, the New York State Energy Research & Development Authority, and the Great Lakes Integrated Sciences & Assessment. We would like to thank T. Gill, N. Nagle, A. Moulton, S. Bohon, and C. Schmertmann for their early feedback and assistance. Thank you!

ACKNOWLEDGMENTS. This work was supported by the State of Louisiana, the American Society of Adaptation Professionals, the New York State Energy Research & Development Authority, and the Great Lakes Integrated Sciences & Assessment. We would like to thank T. Gill, N. Nagle, A. Moulton, S. Bohon, and C. Schmertmann for their early feedback and assistance. Thank you!

1. Mercer JH (1978) West Antarctic ice sheet and CO 2 greenhouse effect: A threat of disaster. *Nature* 271(5643):321.
2. McGranahan G, Balk D, Anderson B (2007) The rising tide: Assessing the risks of climate change and human settlements in low elevation coastal zones. *Environment and Urbanization* 19(1):17–37.
3. Nicholls RJ, Cazenave A (2010) Sea-Level Rise and Its Impact on Coastal Zones. *Science* 328(5985):1517–1520.
4. Strauss BH, Kulp S, Levermann A (2015) Carbon choices determine US cities committed to futures below sea level. *Proceedings of the National Academy of Sciences* 112(44):13508–13513.
5. Neumann B, Vafeidis AT, Zimmermann J, Nicholls RJ (2015) Future Coastal Population Growth and Exposure to Sea-Level Rise and Coastal Flooding - A Global Assessment. *PLOS ONE* 10(3):e0118571.
6. Hauer ME (2017) Migration induced by sea-level rise could reshape the US population landscape. *Nature Climate Change* 7(5):321–325.
7. Davis KF, Battachan A, D'Odorico P, Suweis S (2018) A universal model for predicting human migration under climate change: Examining future sea level rise in Bangladesh. *Environmental Research Letters* 13.
8. De Lellis P, Ruiz Marín M, Porfiri M (2021) Modeling Human Migration Under Environmental Change: A Case Study of the Effect of Sea Level Rise in Bangladesh. *Earth's Future* 9(4). doi:10.1029/2020EF001931.
9. Rigaud KK, et al. (2018) Groundswell.
10. Black R, Bennett SRG, Thomas SM, Beddington JR (2011) Climate change: Migration as adaptation. *Nature* 478:447–449.
11. Clark WA, Maas R (2015) Interpreting migration through the prism of reasons for moves. *Population, Space and Place* 21(1):54–67.
12. Rogers A (1988) Age patterns of elderly migration: An international comparison. *Demography* 25(3):355–370.
13. Gerland P, et al. (2014) World population stabilization unlikely this century. *Science* 346(6206):234–237.
14. Curtis KJ, Schneider A (2011) Understanding the demographic implications of climate change: Estimates of localized population predictions under future scenarios of sea-level rise. *Population and Environment* 33(1):28–54.
15. Hauer ME, et al. (2020) Sea-level rise and human migration. *Nature Reviews Earth & Environment* 1(1):28–39.
16. Marandi A, Main KL (2021) Vulnerable city, recipient city, or climate destination? Towards a typology of domestic climate migration impacts in US cities. *Journal of environmental studies and sciences* 11(3):465–480.
17. Ruggles S, et al. (2021) IPUMS USA: Version 11.0. doi:10.18128/D010.V11.0.
18. Samir K, Lutz W (2017) The human core of the shared socioeconomic pathways: Population scenarios by age, sex and level of education for all countries to 2100. *Global Environmental Change* 42:181–192.
19. Migration induced by sea-level rise could reshape the US population landscape | Nature Climate Change.
20. Molloy R, Smith CL, Wozniak A (2011) Internal migration in the united states. *Journal of Economic perspectives* 25(3):173–96.
21. Findlay AM (2011) Migrant destinations in an era of environmental change. *Global Environmental Change* 21:S50–S58.
22. Chen C, Liu L-M (1993) Joint estimation of model parameters and outlier effects in time series. *Journal of the American Statistical Association* 88(421):284–297.
23. R Core Team (2019) *R: A language and environment for statistical computing* (R Foundation for Statistical Computing, Vienna, Austria) Available at: https://www.R-project.org/.
24. López-de-Lacalle J (2019) *Tsoutliers: Detection of outliers in time series*.
25. Hyndman R, et al. (2019) *forecast: Forecasting functions for time series and linear models* Available at: http://pkg.robjhyndman.com/forecast.
26. Hyndman RJ, Khandakar Y (2008) Automatic time series forecasting: The forecast package for R. *Journal of Statistical Software* 26(3):1–22.
27. Emergency Management and Homeland Security C for (2018) The Spatial Hazard Events and Losses Database for the United States, Version 17.0 [Online Database].
28. Hauer ME (2019) Population projections for US counties by age, sex, and race controlled to shared socioeconomic pathway. *Scientific data* 6(1):1–15.
29. Swanson DA, Schlottmann A, Schmidt B (2010) Forecasting the population of census tracts by age and sex: An example of the hamilton–perry method in action. *Population Research and Policy Review* 29(1):47–63.
30. Wilmoth J, Zureick S, Canudas-Romo V, Inoue M, Sawyer C (2012) A flexible two-dimensional mortality model for use in indirect estimation. *Population studies* 66(1):1–28.
31. Kulp SA, Strauss BH (2019) New elevation data triple estimates of global vulnerability to sea-level rise and coastal flooding. *Nature communications* 10(1):1–12.
32. Sweet WV, et al. (2017) Global and regional sea level rise scenarios for the United States.
33. Kopp RE, et al. (2014) Probabilistic 21st and 22nd century sea-level projections at a global network of tide-gauge sites. *Earth's future* 2(8):383–406.
34. U.S. Fish and Wildlife Service (2012) National wetlands inventory website. U.s. Department of the interior, fish and wildlife service, washington, d.c. Http://www.fws.gov/wetlands/.
35. Millions projected to be at risk from sea-level rise in the continental United States | Nature Climate Change.
36. Hauer ME, Hardy RD, Mishra DR, Pippin JS (2019) No landward movement: Examining 80 years of population migration and shoreline change in Louisiana. *Population and Environment*. doi:10.1007/s11111-019-00315-8.
37. Rogers A (1966) The multiregional matrix growth operator and the stable interregional age structure. *Demography* 3(2):537–544.
38. Hauer M, Byars J (2019) IRS county-to-county migration data, 1990–2010. *Demographic Research* 40:1153–1166.
39. DeWaard J, et al. (2021) User beware: Concerning findings from the post 2011–2012 US internal revenue service migration data. *Population Research and Policy Review*:1–12.
40. Engels RA, Healy MK (1981) Measuring interstate migration flows: An origin—destination network based on internal revenue service records. *Environment and Planning A* 13(11):1345–1360.
41. Franklin RS, Plane DA (2006) Pandora's box: The potential and peril of migration data from the american community survey. *International Regional Science Review* 29(3):231–246.
42. Gross E (2005) Internal revenue service area-to-area migration data: Strengths, limitations, and current trends. *Proceedings of the Section on Government Statistics*, p 2005.
43. DeWaard J, Curtis KJ, Fussell E (2016) Population recovery in new orleans after hurricane katrina: Exploring the potential role of stage migration in migration systems. *Population and environment* 37(4):449–463.
44. Hyndman R, Koehler AB, Ord JK, Snyder RD (2008) *Forecasting with exponential smoothing: The state space approach* (Springer Science & Business Media).
45. Kopp RE, et al. Probabilistic 21st and 22nd Century Sea-Level Projections at a Global Network of Tide-Gauge Sites. *Earth's Future* 2:383–406.